Refinements of the nucleon-exchange transport model for the emission of hard photons and nucleons

S. J. Luke* and R. Vandenbosch
Nuclear Physics Laboratory, GL-10, University of Washington, Seattle, Washington 98195

J. Randrup
Nuclear Science Division, Lawrence Berkeley Laboratory, University of California, Berkeley, California 94720
(Received 16 March 1993)

A previously developed nucleon-exchange transport model for preequilibrium neutron and hard photon emission is extended to include proton emission. Several refinements including diffuse ground-state nucleonic momentum distributions and quantal rather than classical bremsstrahlung production are added. The incorporation of a diffuse momentum distribution improves the reproduction of experimental spectra and multiplicities, particularly at low bombarding energies. Quantal bremsstrahlung enhances the production of high-energy photons. The effect of deceleration of the colliding nuclei during the propagation of the jetting particles through the receptor nucleus is explored. The effect of preequilibrium emission on the evaporation residue and its dependence on entrance channel mass asymmetry is studied. The number of preequilibrium particles emitted is inconsistent with some previous analyses of evaporation residue spectra.

PACS number(s): 25.70.−z

I. INTRODUCTION

A. Motivation

Preequilibrium particle and hard photon emission become increasingly important processes in heavy-ion-induced reactions as the bombarding energy is raised from the low- to intermediate-energy range. Complete fusion becomes relatively improbable, and an increasing fraction of the projectile's mass and momentum escapes as promptly emitted particles. It is important to develop a quantitative understanding of preequilibrium particle emission, both so it can be used as a reaction probe and also to understand its consequences for energy and momentum deposition.

We have previously reported on the development of a model for preequilibrium neutron emission [1]. It was based on a nucleon-exchange transport model [2] and involved the cascade picture employed earlier by Bondorf *et al.* [3]. Similar approaches were subsequently developed by others [4, 5]. The model, which has no fit parameters, had a reasonable degree of success in reproducing preequilibrium particle multiplicities and energy spectra, although it had a tendency to underestimate the hardness of the emission spectra. In a later work the nucleon-exchange transport model was extended to calculate the bremsstrahlung rate from *pn* collisions following nucleon exchange [6].

The present work is an extension of the previously described model [1, 6]. We first describe the incorporation of proton as well as neutron preequilibrium emission. This not only enables us to test the model against available proton energy spectra and multiplicities, but also enables us to calculate some properties of evaporation residues sensitive to preequilibrium particle emission. We then explore refinements and extensions to the model. These include deceleration and rotation of the colliding nuclei during the time of traversal of exchanged nucleons through the receptor nucleus, and the effects of a diffuse rather than a sharp Fermi distribution for the initial ground-state nuclei. Finally, we investigate the possible importance of quantum-mechanical effects on the bremsstrahlung production during *pn* collisions.

B. Synopsis of the model

As the colliding nuclei come into contact, effectively a window opens up between the two nuclei and nucleons can be exchanged between the projectile and target. The size of the window depends upon the impact parameter of the collision. The exchanged nucleons have a velocity in the receptor nucleus determined by the vector coupling of the nucleon velocity in the donor nucleus due to Fermi motion and the velocity of relative motion of the target and projectile at the time of exchange. The exchanged nucleon is then propagated through the receptor nucleus where it can undergo two-body collisions. The model Monte Carlo samples the path distribution for a mean free path determined by the in-medium nucleon-nucleon cross section. The bremsstrahlung production

*Present address: Lawrence Livermore National Laboratory, N-Division L-397, Livermore, CA 94551.

rate is calculated as a perturbation for each p-n collision using classical scattering and radiation theory [7]. Pauli blocking is taken into account in each scattering. Each of the scattering partners is followed until it reaches the nuclear surface where its escape probability is determined from its radial velocity. Quantal reflections and barrier penetration at the surface are taken into account. For those particles which escape, their energy and angle of emission in the laboratory frame is determined by the appropriate transformation. The contributions from exchanges during each time interval of the reaction are accumulated to provide the final energy and angular distributions.

II. EXTENSION OF THE MODEL TO INCLUDE PROTON EMISSION

It had already been necessary to keep track of the nucleon isospin in order to determine the photon production from pn collisions. The propagation of protons through the nucleus is very similar to that of neutrons. Escape at the nuclear surface is determined by calculation of the quantum-mechanical probability for tunneling through a parabolic barrier whose height and curvature is matched to that of the actual nuclear plus centrifugal plus Coulomb potential. After escape the proton is propagated numerically in the Coulomb field of both the donor and receptor nucleus out to a predetermined distance, typically 12 fm for not too heavy systems. Beyond this distance the propagation of the proton is treated analytically using the total Z of the composite system formed. The results are not significantly changed if the switching distance used is increased above the value of 12 fm.

Comparison with proton energy and angular distributions

In our comparison with experimental data we will concentrate on experiments which measure the protons in coincidence with fusion products. This is to avoid the complication of comparing with data which have contamination from sequential decay of projectilelike products of deeply inelastic reactions. Our first comparison is with 20 MeV/nucleon $^{16}O + ^{238}U$ proton spectra taken in coincidence with fission fragments whose folding angle ensures that fission has followed fusion rather than peripheral, small momentum transfer, reactions [8]. Comparisons of proton spectra at representative angles are shown in Fig. 1. The agreement at forward angles for a model with no fit parameters is remarkably good. As one goes back in angle the low-energy part of the spectra becomes dominated by evaporation particles not encompassed in the model, and so one would expect an underprediction of the data. At backward directions, however, a discrepancy emerges, with the calculation overpredicting the number of backward particles. These are induced by nucleons originating in the target and propagating backwards through the projectile. We have noticed a similar discrepancy in model comparisons with a recent inclusive

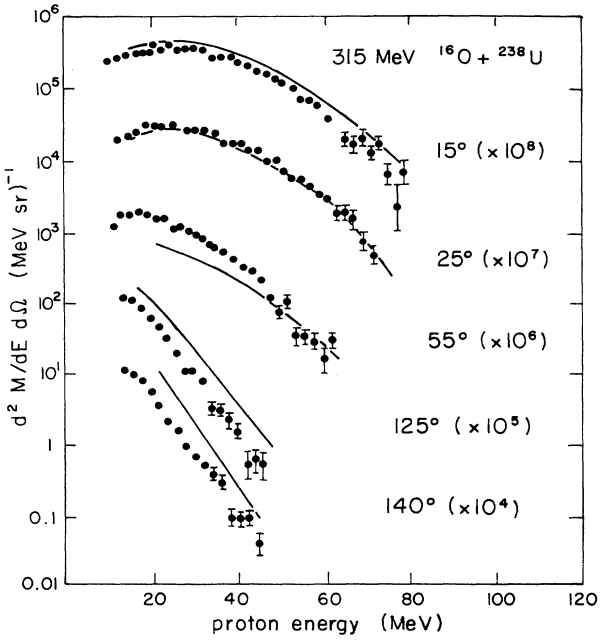

FIG. 1. Comparison of calculated proton spectra with experimental spectra [8] tagged by full momentum transfer fission.

study [9] of neutrons from ^{14}N + Ag at 50 MeV/nucleon. We have not found other examples of such a discrepancy. It is not present in comparisons with data from the same system at 35 MeV/nucleon [10] or in several other exclusive studies of protons in coincidence with evaporation residues.

We compare the model calculations with the data of

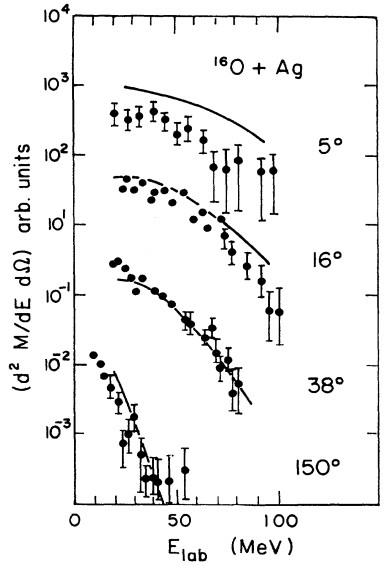

FIG. 2. Comparison of calculated proton spectra for the 30 MeV/nucleon ^{16}O + Ag reaction with experimental spectra [11] tagged by the evaporation residues in the most probable evaporation residue energy bin.

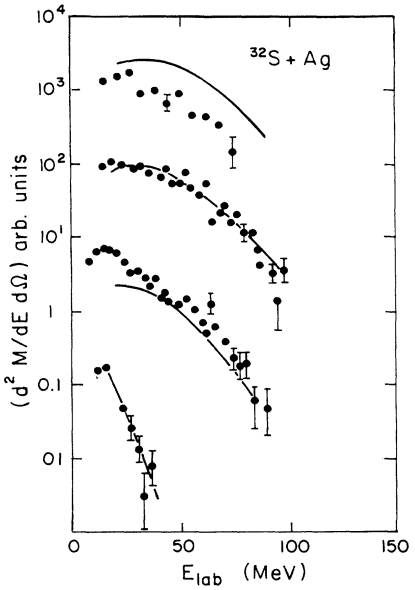

FIG. 3. Comparison of the calculated proton spectra for the 30 MeV/nucleon ^{32}S + Ag reaction with experimental spectra [11] tagged by the most probable evaporation residue energy bin available.

Wada *et al.* [11] for 30 MeV/nucleon ^{16}O and ^{32}S incident on Ag in Figs. 2 and 3. (The normalization of the calculations to the data was made possible by normalization factors made available by R. Wada.) Except perhaps at the most forward angle, the calculations are in good agreement with the experimental data. The comparison is not expected to be quantitative as the reported spectra are for specific residue velocity bins which in the case of ^{32}S do not include the peak of the residue velocity distribution.

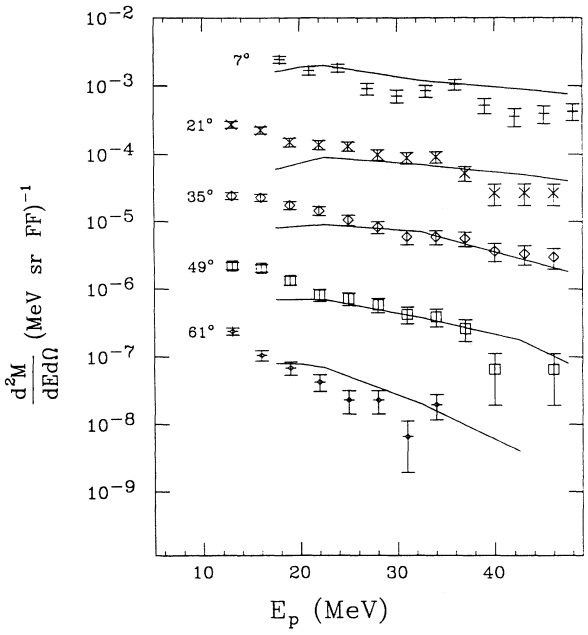

FIG. 4. Comparison of calculated proton spectra for 13.5 MeV/nucleon ^{16}O + Ta reaction with experimental spectra [12] tagged by fission fragments. Spectra at each angle after the smallest have been divided by factors of 10.

We also compare our calculations with results from a recent study [12] of protons in coincidence with fission fragments for 13.5 MeV/nucleon ^{16}O bombardment of Ta in Fig. 4. For this system the fission tag picks out partial waves between 50 and 95. The calculations are in very good agreement with experiment. They also reproduce well the trend with impact parameter as deduced from evaporation residue and fission tagged events for several targets of varying fissility [12].

The model also reproduces fairly well the shape of the energy spectra for the 22.5 MeV/nucleon ^{40}Ar + ^{24}Mg reaction [13]. It does not reproduce the surprisingly soft energy spectra from the 19.7 MeV/nucleon ^{20}Ne + ^{27}Al reaction [14]. These reported spectra are much softer than obtained for the similar ^{28}Si + ^{28}Si reaction at a comparable energy [15]. Leegte *et al.* [16] have shown a comparison of preliminary results of our model with their angle-integrated proton spectrum for 30 MeV/nucleon ^{14}N + ^{232}Th. Subsequent to the time that our results were communicated to them we found an error in a frame transformation in our code and our new results are somewhat reduced in magnitude and are now in excellent agreement with the high-energy part of their spectrum. Our calculation does still overpredict the low-energy proton yield. This comes predominantly in our calculation of the backward jets originating in the target.

III. EFFECTS OF RECEPTOR DECELERATION DURING JET PROPAGATION

In the original implementation of the nucleon exchange preequilibrium emission code [1] the dinuclear motion was frozen during the time that the exchanged nucleons were propagating through the receptor. Gazes [17] has suggested to us that there are some apparent difficulties in the understanding of aspects of the recoil velocity distributions which might be a result of neglecting the deceleration of the relative motion of the target and projectile during the traversal time of the exchanged nucleon through the receptor. He has pointed out that in a mass asymmetric reaction this deceleration will be greatest for the lighter partner, so that potential preequilibrium particles originating in the heavier nucleus will have a larger reduction in their escape probability from the lighter receptor. We have implemented an option in the code which enables us to take into account the effects of deceleration during the propagation of the transferred particle through the receptor. This is achieved by first running the code (with a modest amount of Monte Carlo sampling) and storing the time history of the dinuclear dynamics. The calculation is then repeated, and the stored trajectory then provides the dinuclear motion during the propagation of the final large sample of exchanged particles. The results of including this deceleration effect are in the expected direction, although the effects on the residue velocity are modest. We show in Table I two examples of the comparison of the particle multiplicities and mean energies, one for a reverse kine-

matics reaction and one for a normal kinematics reaction at higher energy. Consider first the $^{40}Ar + {}^{12}C$ example of reverse kinematics. The particle multiplicities for jets originating in either the light or heavy partner are reduced with inclusion of deceleration, and the reduction is largest for jets originating in the heavier (Ar) reactant. The mean kinetic energies of the emitted particles are virtually unaffected, and the mean residue velocity is essentially unchanged. For the $^{14}N + {}^{108}Ag$ reaction the multiplicities for jets originating in the heavier particle are again reduced most, but in this case the heavier reactant is the target rather than the projectile. We have also calculated the hard photon yield for this system, and find a decrease of about a factor of 2 in the cross section for all γ rays over 40 MeV when deceleration is included.

TABLE I. Comparison of preequilibrium particle multiplicity ν, mean laboratory kinetic energy ε (MeV), and residue velocity v_{res} with and without taking into account deceleration during propagation of transferred particle through receptor. The hard photon yield is also compared for the second system.

$^{40}Ar + {}^{12}C$, E/nucleon = 13 MeV, $\ell = 0-20$		
	no deceleration	with deceleration
Neutrons		
Ar→C		
ν	1.39	1.05
ε	17.7	18.4
C→Ar		
ν	1.13	0.98
ε	8	8.2
Protons		
Ar→C		
ν	0.83	0.58
ε	25.8	26
C→Ar		
ν	0.68	0.63
ε	7	7.8
$v_{res}/v_{c.m.}$	1.02	1.02
$^{14}N + {}^{108}Ag$, E/nucleon = 35 MeV, ℓ = 0-140		
	no deceleration	with deceleration
Neutrons		
N→Ag		
ν	1.03	0.80
ε	20.5	26.2
Ag→N		
ν	1.67	1.26
ε	17.2	16.3
Protons		
N→Ag		
ν	0.44	0.44
ε	32.5	37.0
Ag→N		
ν	0.72	0.55
ε	21.4	21.2
Photons		
$d\sigma/d\Omega(E_\gamma > 40$ MeV)	3.1 μb/sr	1.4 μb/sr
$v_{res}/v_{c.m.}$	0.99	0.98

IV. DIFFUSE MOMENTUM DISTRIBUTIONS

The use of diffuse momentum distributions in the calculation of hard photon and nucleon emission in heavy-ion collisions was discussed briefly by Luke *et al.* [10] and will be discussed in more detail in the present work.

A. General considerations

In the original implementation of the nucleon-exchange transport model for the calculation of hard photon [6] and hard nucleon [1] yields, the initial momentum distribution of the nucleons in the nucleus was regarded as a sharp Fermi-Dirac distribution. Though a sharp Fermi-Dirac distribution has been used for the momentum distribution of a zero-temperature noninteracting Fermi-Dirac gas, it is clear that this is not the most appropriate momentum distribution for a realistic nucleus.

Both experimental determination [18–20] and theoretical calculations [21, 22] of the ground-state nucleon momentum distribution have shown that there is a high-momentum tail in the nucleon momentum distribution. This high-energy tail is not reproduced by a zero-temperature Fermi-Dirac distribution. Figure 5 shows a comparison of several k^2-weighted momentum distributions. This figure reveals some interesting aspects of various nucleon momentum distributions. A Hartree-Fock quantum-mechanical calculation gives directly a nucleon momentum distribution exhibiting a high-momentum tail. Diffuse momentum distributions have been used in some Vlasoz-Uehling-Uhlenbeck (VUU) calculations, for example, the calculations of Cassing *et al.* [23]. In

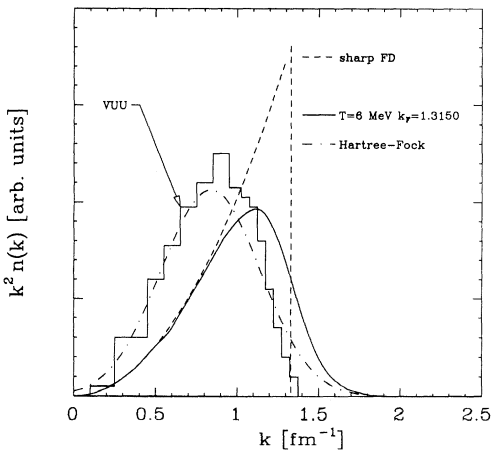

FIG. 5. Various nucleon momentum distributions. The dotted line is the momentum distribution for a zero-temperature Fermi with a Fermi momentum of 1.3305 fm^{-1}. The solid line is the momentum distributions for a finite-temperature Fermi gas with a temperature of 6 MeV with a Fermi momentum of 1.3150 fm^{-1}. The histogram is the nucleon momentum distribution used in the Giessen VUU calculations. The dash-dotted line is the momentum distribution calculated using Hartree-Fock. The VUU and Hartree-Fock momentum distributions are taken from Cassing *et al.* [23]; both of these momentum distributions are for ^{40}Ca.

this case the momentum distributions are calculated by means of a local Thomas-Fermi approximation in the nuclei of interest. This momentum distribution shows nonzero occupation for $k > k_F$, but this contribution is much smaller than predicted by Hartree-Fock calculations. Antonov, Hodgson, and Petkov [22] have shown that the diffuseness in the nucleon momentum distribution can be approximated by a finite-temperature Fermi-Dirac function. The slope of the high-momentum portion of the momentum distribution is a function of the "temperature" chosen for the Fermi-Dirac function. We have found that a "temperature" of 6 MeV approximates the slope of the high-momentum portion of the nucleon momentum distribution [10].

Figure 5 also shows the result of a finite-temperature Fermi-Dirac function for the ground-state momentum distribution using the Fermi energy of 36 MeV adopted in our earlier work. This momentum distribution appears to overestimate the high-momentum tail and underestimate the occupation at low momentum, compared to the Hartree-Fock calculations. This is primarily due to the choice of the Fermi energy in the finite-temperature parametrization of the distribution.

B. Implementation of the diffuse momentum distribution

The diffuseness of the ground-state momentum distribution was included in the nucleon-exchange transport model like a width. The apparent "temperature" (6 MeV) of the ground-state momentum distribution was added in quadrature to the "temperature" of the colliding nuclei at any given time in the reaction process. (This elevated temperature is the consequence of heating the nuclei via one-body dissipation [1].) The Fermi momentum for the diffuse ground-state distribution is downshifted from the value used in a sharp momentum distribution to preserve particle number. The effect of the diffuse momentum distribution is twofold. First, the nucleons in the colliding nuclei can have greater energy, and second, there is a decrease in the amount of Pauli blocking in the receptor nuclei. The first of these effects allows for the yield of higher-energy particles to be increased because of the greater energies involved. This "hardening" of the nucleon-nucleon collisions is much more important for the production of high-energy γ rays than for the emission of hard nucleons because the bremsstrahlung emission rate for a γ ray of a particular energy increases with increased energy in the nucleon-nucleon system. In the case of nucleon emission the multiplicity of the emitted nucleons depends on the mean free path of the nucleons in the nuclear media. The mean free path of nucleons in a nucleus is relatively independent of the energy of the nucleon above approximately 30 MeV, and so there will be less of an effect of the diffuseness of the momentum distribution on the nucleon emission spectrum. The second of these effects causes an overall increase in the number of emitted particles because of the opening up of the final-state phase space. This should have large effects on both the production of high-energy γ rays and the emission of hard nucleons, because it makes the in-medium nucleon-nucleon collisions more probable.

The magnitude of the effect of the inclusion of a diffuse ground-state momentum distribution on the calculated emission of hard photons and nucleons depends upon bombarding energy. We examine first the effect on a reaction at a fairly high bombarding energy, 35 MeV/nucleon. This is illustrated in Fig. 6. As this figure shows, the effect of the diffuse momentum distribution on γ-ray emission is large. The "hardness" of the calculated spectrum has increased as has the overall yield of the γ rays. The increased hardness (as was discussed above) is a consequence of the higher energies available in the nucleon-nucleon collision. The overall increase of the yield, on the other hand, is the result of decreased Pauli blocking at low momenta. Figure 6 also shows that there is a modest increase in the calculated yield of nucleon emission; however, the slope of the spectra are about the same. These results are consistent with the expectations discussed above. The effects at lower bombarding energies are larger, particularly on the nucleon emission. For example, at 14 MeV/nucleon the preequilibrium proton multiplicity is enhanced by a factor of 4. This relatively larger effect at low bombarding energies is the result of exploiting the tail of the momentum distribution when coupled to the relative motion of the colliding nuclei to achieve sufficient energy for the nucleons to escape the nucleus. At higher bombarding energies not only is the relative motion larger, but also the colliding nuclei achieve a higher real temperature due to energy dissipation which makes a sizable contribution to the diffuseness of the momentum distribution. Therefore, the diffuseness of the ground-state momentum distribution is a relatively small perturbation to the diffuseness of the nuclei after the nuclei interact.

There is, however, a problem with the incorporation of a diffuse momentum distribution as has been described here. Because of the diffuseness in the ground-state momentum distribution, it is possible for γ rays (and nucleons) to be emitted spontaneously. This spurious emission is the result of the same considerations which lead to enhancement in the emission of the high-energy particles in the first place. The diffuseness in the momentum distribution results in some probability for the ground-state nuclei to have sufficient energy to emit fairly high-energy γ rays and particles without any dynamical considerations. The most important of these considerations is the coupling of the velocities of the individual nucleons to the relative velocity of the colliding nuclei. The spurious emission of γ rays is further enhanced by the fact that the diffuseness in the momentum distribution opens up phase space at low momentum for the nucleons to scatter into after the production of the photons. To try to correct for this background the calculation for the emission of the γ rays was run identically to the normal manner, but the coupling of the nucleons to the relative motion of the nuclei was turned off. This provided an estimate of the spurious contribution. The result for the emission of γ rays shown in Fig. 6 is the result of taking this background into account. The code is run including the coupling to the relative motion and then without coupling to the relative motion. The calculation without

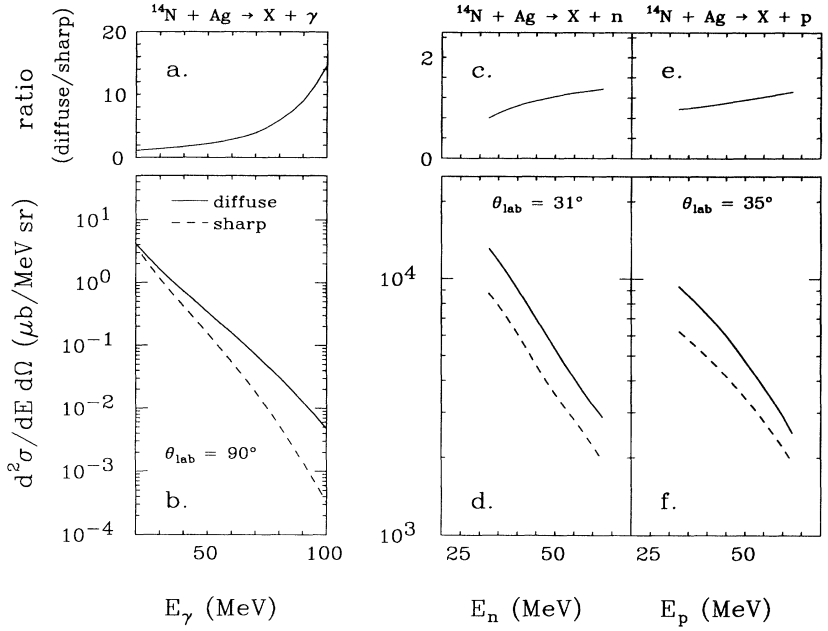

FIG. 6. Effect of diffuse ground-state momentum distribution on the high-energy photon production and nucleon emission in ^{14}N + Ag at 35 MeV/nucleon for a laboratory angle of 90°. Panels (a), (c), and (e) show the ratio of the yield from a diffuse momentum distribution to that from a sharp momentum distribution as a function of energy. Panels (b), (d), and (f) show the calculated spectra. The solid lines are the result of the calculation with a diffuse momentum distribution. The dashed lines are the result of the calculation with a sharp momentum distribution. The photon yield is calculated using classical bremsstrahlung.

coupling is subtracted from the calculation with the coupling to yield the final result. The dashed lines in Fig. 7 show the magnitude of the calculated background for γ rays and nucleons emitted in the reaction ^{14}N + Ag at 35 MeV/nucleon. As this figure shows, the background subtraction due to the spurious emission is more important in the emission of γ rays than for the emission of nucleons. This is expected because the emission of high-energy nucleons depends a great deal on the amount of coupling of the nucleon motion with the relative motion of the nuclei in the collision.

One might be concerned that a background correction described above should also be performed for calculations using a sharp momentum distribution since the transfer of nucleons during the course of the reaction process causes a heating of the receptor nuclei. The resultant hotter nuclei have a diffuseness in their momentum distributions which is a function of the temperature in the nucleus. This, in contrast to the case of the diffuse ground-state momentum distribution, is a physical tem-

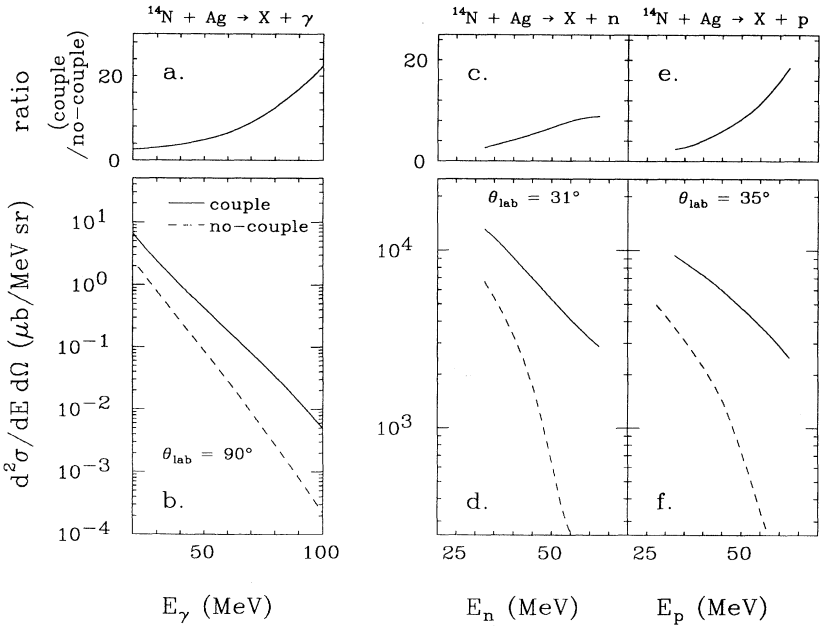

FIG. 7. Effect of coupling of the nucleon velocities to the relative motion of the nuclei on γ-ray production and nucleon emission for ^{14}N + Ag at 35 MeV/nucleon for a laboratory angle of 90°. Panels (a), (c), and (e) show the ratio of the calculation which includes coupling with diffuse momentum distribution to the result without coupling to the relative motion. Panels (b), (d), and (f) show the results of the calculation of the absolute photon and nucleon emission spectra for coupling (solid) and no coupling (dashed) of the nucleons to the relative motion of the nuclei. The photon yield is calculated using classical bremsstrahlung.

perature and, therefore, none of the particles produced are spurious. Therefore, a background correction should not be performed.

V. QUANTUM-MECHANICAL BREMSSTRAHLUNG

A. General considerations of bremsstrahlung production

Recently, there have been several new attempts to calculate the bremsstrahlung production in nucleon-nucleon collisions. There are two major methods used to calculate the bremsstrahlung rate: potential models [24–27] and covariant models [28, 29]. The major difference between these two models is the philosophy each takes in solving the perturbation calculation. The potential model calculations take the view that the bremsstrahlung rate may be calculated using the formalism of scattering theory, while the covariant method solves the perturbation diagrams for the bremsstrahlung production directly. Though the specifics of the two methods differ, the results of the calculations are similar. Both Nakayama [26] and Schäfer *et al.* [29] have shown that there seems to be an enhancement of the bremsstrahlung rate when quantum-mechanical effects, such as charged meson exchange, were included in the calculations. (The enhancement of the bremsstrahlung rate due to meson exchange was first demonstrated in 1973 by Brown and Franklin [25].) They have also shown that this enhancement seems to be more important near the kinematic limit. This might imply that the inclusion of the quantum-mechanical bremsstrahlung effects would be much more important in the case of proton induced reactions than in the heavy-ion reactions under consideration in the present work because the γ rays produced near the kinematic limit for the heavy-ion reactions are not experimentally accessible. From the examination of the bremsstrahlung calculations of Schäfer *et al.* [29], Nakayama [26], and Herrmann, Speth, and Nakayama [27] we thought it was desirable to include the contribution of meson-exchange current in the refined model in order to have a more realistic model for hard photon production. It was also clear that the contribution to the bremsstrahlung rate would have to be included in an *ad hoc* manner since the model treats the nucleon-nucleon collisions in a classical manner. Fortunately, this task was made more tractable recently by the fact that Schäfer *et al.* provided a parametrization of the results of a full quantum-mechanical treatment of bremsstrahlung production in a simple functional form.

B. Implementation of quantum-mechanical bremsstrahlung

Implementing the parameterization of Schäfer *et al.* [29] into the nucleon-exchange transport model involved additional consideration for two reasons. First, Schäfer *et al.* only give a parametrization for the total emission cross section, whereas a parametrization for the emission probability is required for the model. Second, Schäfer *et al.* only gave a parametrization of the angle-integrated bremsstrahlung production cross section. In the calculation of the bremsstrahlung yield in the nucleon-exchange transport model it is necessary to have the double differential probability for the photon production. This is because the angular distribution of the emitted photons is a function of the final state of the nucleons after γ-ray emission. The first of these problems is solved by dividing by the empirical nucleon-nucleon cross section [30] to obtain the angle-integrated probability for producing bremsstrahlung in a p-n collision. The second of these problems is a little more subtle, because of the way in which the model is used to calculate the double differential probability for γ-ray production [31]. This problem is dealt with as follows. The model calculation for γ-ray production in a p-n collision is integrated over solid angle yielding an angle-integrated bremsstrahlung probability. By dividing the parametrization of Schäfer *et al.* by this quantity and then multiplying by the double differential probability for photon production in the model [6] an event-by-event correction of the differential γ-ray yield is obtained. This argument assumes that the angular dependence of the quantum-mechanical and classical models for bremsstrahlung emission are the same. This seems to be a reasonable approximation in the nonrelativistic limit, and this is the assumption made by Schäfer *et al.* Although this is a reasonable approximation, it may not be entirely accurate because Herrman, Speth, and Nakayama [27] have shown that at higher pn energies there may be a quadrupole term in the photon angular distribution, whereas the purely classical calculation only produces a dipole angular distribution.

C. Effect of quantum-mechanical bremsstrahlung on calculated photon yields

As was mentioned above, the inclusion of quantum-mechanical bremsstrahlung should have the greatest effect near the kinematic limit in the c.m. system of the colliding nucleons. This energy regime is rarely accessible in intermediate energy heavy-ion collisions because of experimental limitations. However, this region of phase space is accessible in proton-nucleus collisions. Figure 8 shows a comparison of the photon yield calculated using quantum-mechanical and classical bremsstrahlung for p + Au at 34 and 72 MeV and p + Pb at 104 MeV.

As Fig. 8 shows, the effect of the inclusion of quantum-mechanical bremsstrahlung is small for p + Au at 34 MeV. This is not surprising since Schäfer *et al.* show that the magnitude of the enhancement of the bremsstrahlung yield from quantum-mechanical bremsstrahlung depends on the center-of-mass kinetic energy of the p-n pair. At the lowest energies they considered (90 MeV) the enhancement is a great deal less than at the highest energies. This may be understood in a very simple manner. The effect of quantum-mechanical bremsstrahlung, specifically the exchange current, has a threshold. This threshold is the mass of the lightest exchanged meson, which, of course, is the pion mass. For energies in the nucleon-nucleon system below the pion mass the effect of exchange currents to the bremsstrahlung production is small, as Schäfer *et al.* show. So the result of very

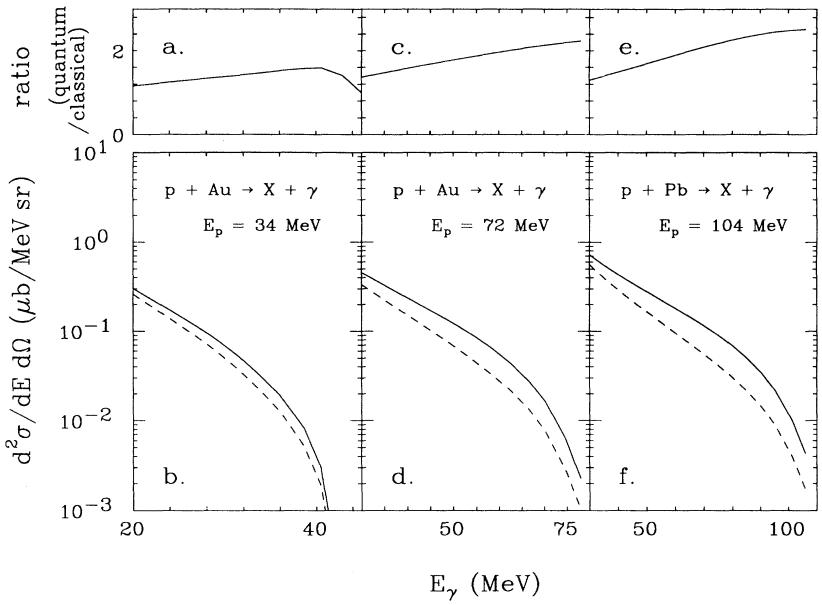

FIG. 8. Effect of quantum-mechanical bremsstrahlung on the emission of hard photons in p + Au at 34 and 72 MeV and p + Pb at 104 MeV. Panels (a), (c), and (e) show the ratio of the yield calculated using quantum-mechanical bremsstrahlung to the yield for classical bremsstrahlung for each of the reactions. Panels (b), (d), and (f) show the absolute yields for the two calculations.

little enhancement of the hard photon yield in p + Au at 34 MeV is not that surprising. This argument is further supported by the comparison of the photon yield at incident proton energies of 72 and 104 MeV. As Fig. 8 shows, the effect of the inclusion of quantum effects increases with the incident energy of the proton. The effect of replacing classical bremsstrahlung with quantum-mechanical bremsstrahlung on γ rays produced in ^{14}N + Ag at 35 MeV/nucleon is shown in Fig. 9. As this figure shows, the effect of the inclusion of quantum-mechanical bremsstrahlung is about the same in the heavy-ion case as in the case of proton-induced reactions.

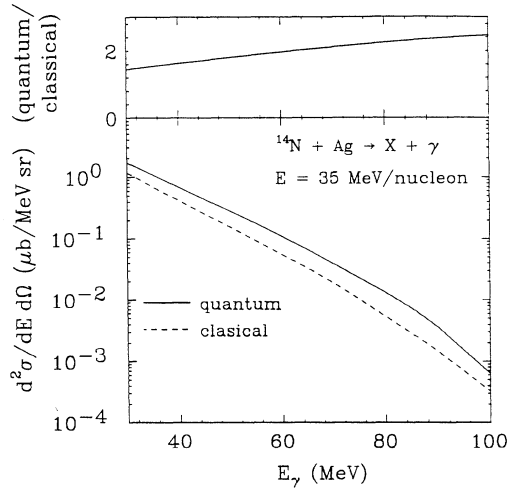

FIG. 9. Effect of quantum-mechanical bremsstrahlung on the emission of hard photons in ^{14}N + Ag at 35 MeV/nucleon. Panel (a) shows the ratio of the yield calculated using quantum-mechanical bremsstrahlung to the yield for classical bremsstrahlung. Panel (b) shows the absolute yields for the two calculations.

VI. COMPARISON OF CALCULATED AND EXPERIMENTAL γ-RAY YIELDS

A. Inclusive measurements

The effect of including diffuse momentum distributions on the production of high-energy γ rays in heavy-ion reactions was first presented by Luke *et al.* [10] and is shown in Fig. 10 for ^{14}N + Ag at 35 MeV/nucleon. Also shown in this figure is the effect of the inclusion of quantum-

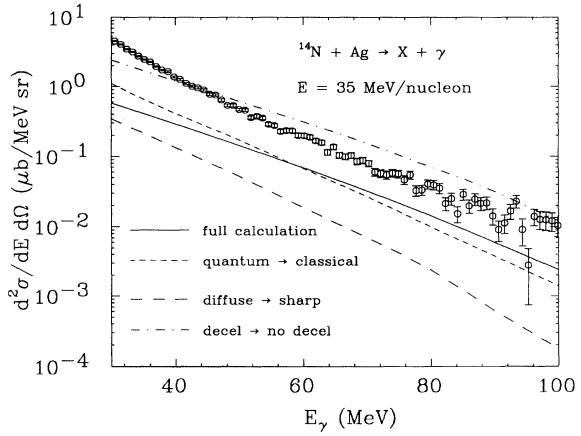

FIG. 10. Comparison of the 90° inclusive spectrum of high-energy γ-ray production in ^{14}N + Ag at 35 MeV/nucleon [10] with model calculations. The solid line is the result of the calculation using all of the refinements discussed in the text (quantum-mechanical bremsstrahlung, diffuse ground-state momentum distributions, and the deceleration option). The short dashed, long dashed, and the dash-dotted lines are the result of replacing quantum-mechanical bremsstrahlung with classical bremsstrahlung, diffuse momentum distribution, with sharp momentum distribution, and deceleration with no deceleration, respectively.

mechanical bremsstrahlung on the γ-ray yield. As this figure shows it is necessary to include a diffuse ground-state momentum distribution to reproduce the observed experimental yield. The effect of the diffuse ground-state momentum distribution has a larger effect than the inclusion of quantum-mechanical bremsstrahlung with a sharp momentum distribution. The calculation which uses a diffuse ground-state momentum distribution and quantum-mechanical bremsstrahlung with no deceleration overpredicts the data a factor of 2 or so above 40 MeV.

Figure 11 shows the result of the calculations for more symmetric systems, ^{40}Ar + Ca at 30 MeV/nucleon [34] and ^{36}Ar + ^{27}Al at 85 MeV/nucleon [35]. This figure shows some very interesting aspects about the calculations. As was mentioned above, the relative importance of a diffuse ground-state momentum distribution decreases as the energy of the projectile increased. This effect is clearly seen in Fig. 11 where the enhancement due to a diffuse distribution is much greater for the system at 30 MeV/nucleon than for the system at 85 MeV/nucleon. Our calculations show that the agreement with the data when both a diffuse momentum distribution and quantum-mechanical bremsstrahlung are used is between a factor of 4 and 9. Both Figs. 10 and 11 show that the general agreement of the calculations with the data is fairly good, especially for a model with no fit parameters.

Figure 12 shows the comparison of the calculated γ-ray yield in proton-induced reactions with the experimental data at 34 MeV [31], 72 MeV [32], and 104 MeV [33]. As this figure shows the agreement between the experiment and the calculations is very good for high γ-ray energies. At lower γ-ray energies the agreement between the calculation and the data is not so good, particularly at a proton energy of 34 MeV. This might suggest that there are other mechanisms involved in the production of

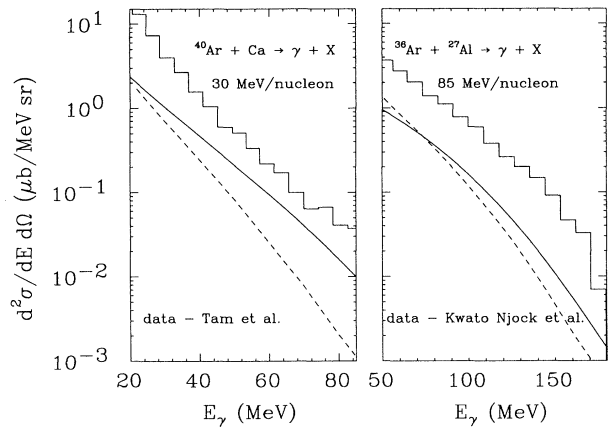

FIG. 11. Comparison of the 90° inclusive spectrum of high-energy γ-ray production in ^{40}Ar + Ca at 30 MeV/nucleon [34] and ^{36}Ar + ^{27}Al 85 MeV/nucleon [35] with model calculations. The solid line is the result of the calculation using all of the refinements discussed in the text. The dashed line has a sharp rather than a diffuse momentum distribution. The data are shown as histograms.

γ rays at these energies. At these low bombarding there is a relatively high probability that γ rays might be produced by a direct-semidirect (DSD) mechanism. However, Luke [31] has shown that the contribution from this mechanism is rather small at 34 MeV at least when the contribution is calculated with a primitive model in which there is no coupling to the continuum states, inclusion of $E2$ radiation, or any multistep process. Since the discrepancy persists for all of the proton energies considered and the importance of a DSD mechanism would decrease with increasing energy, the inability of the model to reproduce the low-energy yield might suggest that there is more physics involved in the γ-ray production than is included in the model. One possible source of enhancement of γ-ray yield at low γ energies might be bremsstrahlung involving more than two nucleons i.e., the incident proton interacting with correlated nucleons in the target nuclei. Another possible source of γ-ray production at these lower energies might be γ-ray production through a DSD multistep process. Further work is required to clarify this situation.

B. Exclusive measurements

As an example of the comparison of our model for photon production with exclusive data we have performed calculations for the Xe + Au system at 44 MeV/nucleon recently studied by Migneco *et al.* [36]. They have used as an impact parameter tag the light charged particle multiplicity, making the assumption that there is a monotonic anticorrelation between the impact parameter b and the multiplicity. The dependences of multiplicity and of the slope parameter characterizing the laboratory system photon spectrum are compared with the experimental data in Fig. 13. The agreement at the smaller impact parameters, where the dependence on impact parameter is weak, is reasonable. For large impact parameters the calculation shows a sharper drop than the experiment. This may simply reflect the neglect of fluctuations in the light charged particle multiplicity with impact parameter.

We also performed calculations for exclusive photon production for the system ^{40}Ar + ^{51}V at 65 MeV/nucleon recently studied by Reposeur *et al.* [37]. Reposeur *et al.* measured high-energy γ rays in coincidence with light charged particles. They obtained double differential cross sections for the photon production as a function of the centrality of the collision. They determined the centrality of the collision by the midrapidity charge representation of Ogilvie *et al.* [38]. Reposeur *et al.* further assumed that the ^{40}Ar + ^{51}V was sufficiently symmetric that the formalism of Ogilvie *et al.* was applicable for their slightly asymmetric system. Reposeur *et al.* reported double differential cross sections for four classes of reactions: central, midcentral, midperipheral, and peripheral. We have used the impact parameter distributions in Fig. 7 of Ref. [38] together with the constraint that $\sigma(b)$ is proportional to b to deduce the (overlapping) b distribution for each gate. We compare the results of our calculations with the experimental data and previous Boltzmann-Uehling-Uhlenbeck (BUU) calculations in

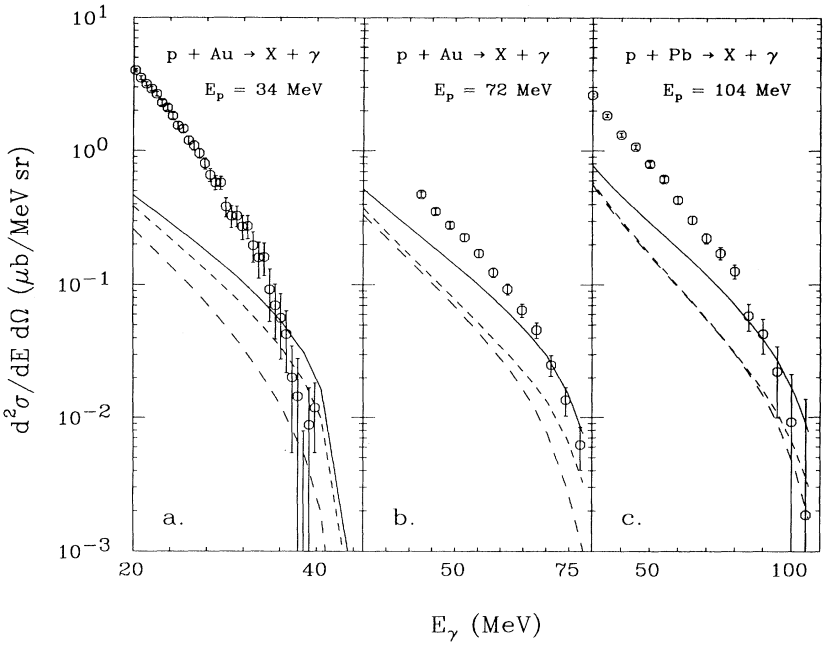

FIG. 12. Comparison of the 90° inclusive spectrum of high-energy γ-ray production in p + Au at 34 and 72 MeV and p + Pb at 104 MeV with model calculations. The data are from Luke [31], Kwato Njock *et al.* [32], and Clayton *et al.* [33]. The solid line is the result of the calculation using the nucleon-exchange transport model with the full calculation for proton-induced reactions (quantum-mechanical bremsstrahlung and diffuse ground-state momentum distribution). The short dashed line is the result of the calculation changing the diffuse momentum distribution to a sharp distribution. The long dashed line is the result of the calculation with classical bremsstrahlung and sharp momentum distribution.

Fig. 14. Our model systematically underpredicts the data somewhat, but gives a good representation of the impact parameter dependence of the slope and yield. Our results are generally in better agreement with the data than the BUU calculations, particularly with regard to the impact parameter dependence of the slope. The latter comparison is shown in Table II, where it can be seen that our impact parameter dependence of the slope is in excellent agreement with experiment.

VII. EVAPORATION RESIDUE VELOCITY DISTRIBUTIONS

There have been a number of studies of the widths and centroids of evaporation residue velocity distributions, some of which have led to surprising conclusions. Morgenstern *et al.* [39] have studied residues for a number of systems of differing mass asymmetry in the entrance channel. From these and other results they suggest that the probability of emission depends on the velocity of the lighter of the two reaction partners, relative to the c.m. velocity, rather than the relative velocity of the partners. Stephans *et al.* [40] and Gonin *et al.* [41] have come to similar conclusions. Pienkowski *et al.* [42] measured the velocity distributions as a function of angle and decomposed these into parallel and perpendicular velocity distributions. From these they deduced the number of

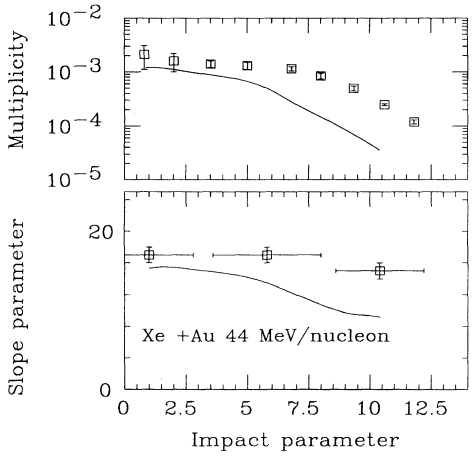

FIG. 13. Comparison of the experimental hard photon multiplicity and slope parameters of Migneco *et al.* [36] for Xe + Au at 44 MeV/nucleon with the present model calculations, using diffuse momentum distributions, quantum-mechanical bremsstrahlung and the deceleration option.

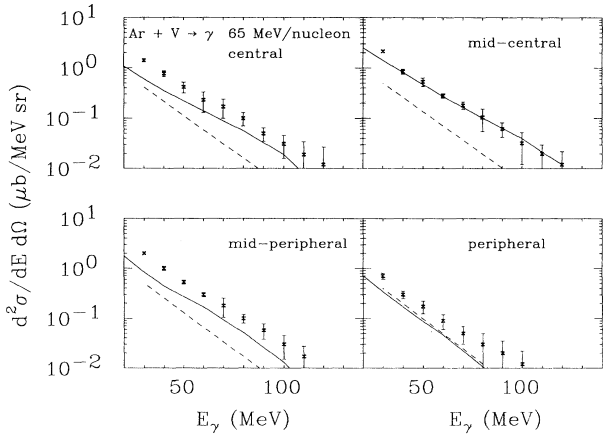

FIG. 14. Comparison of the model calculations, using quantum-mechanical bremsstrahlung, diffuse ground-state momentum distributions, and the deceleration option with the exclusive γ-ray emission data of Reposeur *et al.* [37] for Ar + V at 65 MeV/nucleon. The solid lines are the result of the full calculations; the dashed lines are the results of the BUU calculations taken from Reposeur *et al.*

TABLE II. Comparison of γ-ray slope parameters (in MeV) for ^{40}Ar + ^{51}V at 65 MeV/nucleon for various classes of impact parameter. The values of the experimental and BUU slope parameters are from Reposeur *et al.* [37]. The slope parameters for the present calculations are the result of calculations using diffuse momentum distributions, quantum-mechanical bremsstrahlung, and the deceleration option.

	E_0 (Experiment)	E_0 (Present calculations)	E_0 (BUU)
Central	19.3 ± 0.7	20.6	15.5
Midcentral	18.7 ± 0.4	20.0	15.4
Midperipheral	17.6 ± 0.4	17.0	14.8
Peripheral	14.5 ± 0.9	13.0	14.3

preequilibrium particles originating in the target and projectile.

Let us first consider in detail the study of Morgenstern *et al.* [39]. They have reported the residue velocity distribution at small angles for ^{40}Ar bombardment of ^{12}C and ^{40}Ca and for ^{20}Ne bombardment of ^{27}Al. These provide examples of a heavy projectile on a light target, a heavy projectile on a target of equal mass, and a light projectile on a heavy target. They find that the centroid of the velocity distribution is less than that of the center of mass (which would be the velocity of the compound nucleus formed if there were no preequilibrium particles) for a light projectile on a heavier target. Conversely, they find a centroid velocity higher than the c.m. velocity for a heavy projectile on a lighter target. They furthermore attempt to decompose the velocity distributions into three components: complete fusion, incomplete fusion with mass loss from the projectile, and incomplete fusion with mass loss from the target. In our judgment this is not possible to do quantitatively for symmetric and near symmetric systems. For such systems one is very sensitive to the assumed velocity width arising from evaporation from the composite nucleus. This width is sensitive to the masses of the evaporated particles and to their angular distributions. For example, Morgenstern *et al.* [39] decompose the symmetric residue velocity distribution for the 520 MeV Ar + Ca reaction into a complete fusion component comprising 80% of the events and two incomplete fusion components comprising the remainder of the residue events. Our nucleon exchange model, as well as systematics of preequilibrium particle multiplicities, would predict about four particles. Assuming a Poisson distribution, one would expect only 2% complete fusion, rather than 80% suggested by Morgenstern *et al.* An alternative interpretation of the residue velocity distribution in terms of mostly incomplete fusion is possible since for this nearly symmetric system one expects the residue velocity distribution to be centered at the same velocity as the center of mass for complete fusion or incomplete fusion. Morgenstern *et al.* assumed that incomplete fusion was associated with considerable mass loss from *either* the target *or* the projectile, rather than the more probable loss of comparable mass from *each* fragment for this mass-symmetric system.

We can use the nucleon-exchange transport model to calculate the mean residue velocity. We have done this for the three previously mentioned reactions for which Morgenstern *et al.* report residue velocity distributions. For the ^{20}Ne + ^{27}Al reaction we interpolate between results [43] at about 11 and 15 MeV/nucleon to obtain a value at 13 MeV/nucleon corresponding to the argon bombarding energy. We show in Fig. 15 the calculated and experimental ratios of the observed residue velocity centroid to the c.m. velocity. The calculations include the effect of the deceleration of the fragments during traversal of the receptor nucleus, although this process has a negligible effect on the residue velocity for these systems. Our model reproduces the trend of the data, but underestimates the magnitude of the residue velocity shifts.

The qualitative behavior can be understood from very simple considerations based on the Fermi jet picture. If one neglects scattering in the receptor and potential barriers for escape, the number of preequilibrium particles originating in the target and projectile will be equal independent of entrance channel mass asymmetry. In this limit the ratio of residue velocity to the c.m. velocity is given by

$$\frac{v_{\rm res}}{v_{\rm c.m.}} = \frac{(A_P - n_P)(A_P + A_T)}{A_P\,(A_P + A_T - n_P - n_T)}, \tag{1}$$

where A_P and A_T are the projectile and target masses and n_P and n_T are the preequilibrium particles origi-

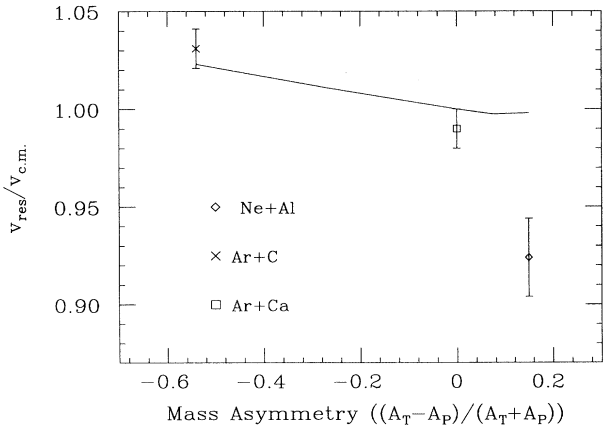

FIG. 15. Comparison of experimental and calculated (solid curve) ratios of residual velocity to center-of-mass velocity for several systems at 13 MeV/nucleon but with different entrance channel mass asymmetry. The experimental data are from Morgenstern *et al.* [43, 39].

nating in the projectile and target. If $n_P = n_T$, then $v_{res}/v_{c.m.} < 1$ for $A_P < A_T$ and > 1 for $A_P > A_T$. The condition for $v_{res}/v_{c.m.} = 1$ is then $n_P/A_P = n_T/A_T$. Thus the experimental dependence of the residue velocity on mass asymmetry is consistent with the Fermi jet expectation of more nearly equal numbers of preequilibrium particles originating from the two reaction partners.

The underestimation of the reduction in $v_{res}/v_{c.m.}$ for large mass asymmetry may arise from several causes. The direction of the effect would be consistent with an overestimation of the number of backward preequilibrium particles as mentioned earlier. It may also reflect the mass and momentum loss associated with complex particle (d, t, α) emission or contributions of massive transfer breakup fusion [44] mechanisms.

We do not feel it is possible to compare our model calculations with data at higher bombarding energy because of biases in the data analyses. The reason is that at high energies there is a large overlap in fusion residue masses with those from projectilelike and targetlike products of binary exit channels. For example, Pienkowski *et al.* [42] have reported $v_{res}/v_{c.m.}$ values at 30–32 MeV/nucleon. These values were, however, extracted from the small fraction (<10%) of the events with Z larger than that of the target. This can lead to a bias in the $v_{res}/v_{c.m.}$ values, as can be seen from Fig. 1 of [42] and from the work of Gonin *et al.* [41].

VIII. CONCLUSIONS

We have extended our nucleon-exchange transport model to also include proton emission in addition to neutron emission. This extension is relatively straightforward, requiring only additional effects of the Coulomb barrier for the escaping protons and the effect of the Coulomb potentials of both donor and receptor nuclei on the outgoing proton. The multiplicity of the preequilibrium protons is lower than that of the neutrons.

We have also incorporated the effect of the known diffuse momentum distributions of the nucleons in the nuclear ground-state. This has been done in a somewhat *ad hoc* manner since it goes beyond the basic one-body nature of the model. The diffuseness used in our calculations is based on simulating the experimental ground-state nucleon momentum distribution rather than by fitting preequilibrium particle emission spectra. It is therefore gratifying to find that the high-energy slopes of the calculated neutron, proton, and γ-ray emission spectra are in reasonable agreement with experiment. This extension is most important for low bombarding energy and for more asymmetric systems at a given bombarding energy, as it increases the multiplicity and hardens the spectra most in these circumstances. For higher bombarding energies and more symmetric systems energy dissipation at the early stages of the collision leads to hot nuclei with diffuse momentum distributions which dominate the contribution from the corrections to the diffusivity of the ground-state momentum distribution.

We have also investigated changes in the expected *pn* nucleon-nucleon bremsstrahlung due to both the aforementioned diffuse momentum distributions and quantum-mechanical effects on the elementary production mechanism. The latter had been treated classically in our earlier work [6]. Brown and Franklin [25] and more recently Nakayama [26] and Schäfer *et al.* [29] have shown that quantum-mechanical effects are most important at higher nucleon-nucleon energies and for photons near the kinematic limit. The enhancements are typically less than a factor of 2. When incorporated in our transport model the effects from quantum-mechanical bremsstrahlung are most important for proton-induced reactions where it is possible to measure the photon emission near the kinematic limit and for heavy-ion reactions at higher bombarding energies.

We have pursued a suggestion that deceleration of the partners in the heavy-ion reaction during the transit time of an exchanged nucleon may modify the emission probability more for jets originating from the heavier reaction partner than for those originating from the lighter partner. The results obtained are in the direction expected, but their effect on residue velocity is modest. Predictions of mean residue velocities exhibit the correct trend with mass asymmetry of the entrance channel but considerably underestimate the magnitude of the dependence. This underestimation is attributed to the large amounts of momentum being carried away by composite particles, particularly α particles. These composite particles may arise from massive transfer or breakup-fission mechanisms, as well as from coalescence mechanisms.

[1] J. Randrup and R. Vandenbosch, Nucl. Phys. **A474**, 219 (1987).

[2] J. Randrup, Nucl. Phys. **A327**, 490 (1979); **A383**, 468 (1982); T. Døssing and J. Randrup, *ibid.* **A433**, 215 (1985).

[3] J. P. Bondorf, J. N. De, G. Fai, A. O. T. Karvinen, B. Jakobsson, and J. Randrup, Nucl. Phys. **A333**, 285 (1980).

[4] S. Leray, G. La Rana, C. Ngo, M. Barranco, M. Pi, and X. Vinas, Z. Phys. A **320**, 383 (1985).

[5] S. Bhattacharya, K. Krishan, S. K. Samaddar, and J. N. De, Phys. Rev. C **37**, 2916 (1988).

[6] J. Randrup and R. Vandenbosch, Nucl. Phys. **A490**, 418 (1988).

[7] K. Nakagama and G.F. Bertsch, Phys. Rev. C **34**, 2190 (1986).

[8] T. C. Awes, G. Poggi, C. K. Gelbke, B. B. Back, B. G. Glagola, H. Breuer, and V. F. Viola, Jr., Phys. Rev. C **24**, 89 (1981).

[9] H. R. Schelin *et al.*, Nucl. Sci. Eng. **113**, 184 (1993).

[10] S. J. Luke, R. Vandenbosch, W. Benenson, J. Clayton, K. Joh, D. Krofcheck, T. K. Murakami, and J. D. Stevenson, Phys. Rev. C **47**, 1200 (1993).

[11] R. Wada *et al.*, Phys. Rev. C **39**, 497 (1989).

[12] D. Prindle, R. Vandenbosch, S. Kailas, A. Charlop, and C. Hyde-Wright, Phys. Rev. C (in press).

[13] A. Malki *et al.*, Z. Phys. A **339**, 283 (1991).

[14] K. A. Griffioen, E. A. Bakkum, P. Decowski, R. J. Meijer, and R. Kamermans, Phys. Rev. C **37**, 2502 (1988).

[15] G. Nebbia *et al.*, Phys. Rev. C **45**, 317 (1992).

[16] H. K. W. Leegte, A. L. Boonstra, J. D. Hinnefeld, E. E. Koldenhof, R. H. Siemssen, K. Siwek-Wilczyńska, Z. Sosin, J. Wilczyński, and H. W. Wilschut, Phys. Rev. C **46**, 991 (1992).
[17] S. B. Gazes (private communication).
[18] R. D. Amado and R. M. Woloshyn, Phys. Lett. **62B**, 253 (1976); Phys. Rev. Lett. **36**, 1435 (1976); Phys. Rev. C **15**, 2200 (1977).
[19] H. J. Weber and L. D. Miller, Phys. Rev. C **16**, 726 (1977).
[20] P. E. Sokol, R. N. Silver, and J. W. Clark, in *Momentum Distributions*, edited by R. N. Silver and P. E. Sokol (Plenum, New York, 1989).
[21] I. Sick, in *Momentum Distributions*, edited by R. N. Silver and P. E. Sokol (Plenum, New York, 1989).
[22] A. N. Antonov, P. E. Hodgson, and I. Zh. Petkov, *Nucleon Momentum and Density Distributions in Nuclei* (Clarendon, Oxford, 1988).
[23] W. Cassing, V. Metag, U. Mosel, and K. Niita, Phys. Rep. **188**, 363 (1990).
[24] V. R. Brown, Phys. Lett. **32B**, 259 (1970).
[25] V. R. Brown and J. Franklin, Phys. Rev. C **8**, 1706 (1973).
[26] K. Nakayama, Phys. Rev. C **39**, 1475 (1989).
[27] V. Herrmann, J. Speth, and K. Nakayama, Phys. Rev. C **43**, 394 (1991).
[28] T. S. Biró, K. Niita, A. L. De Paoli, W. Bauer, W. Cassing, and U. Mosel, Nucl. Phys. **A475**, 579 (1987).
[29] M. Schäfer, T. S. Biró, W. Cassing, U. Mosel, H. Nifenecker, and J. A. Pinston, Z. Phys. A **339**, 391 (1991).
[30] K. Chen, Z. Frainkel, G. Friedlander, J. R. Grover, J. M. Miller, and Y. Shimamoto, Phys. Rev. **166**, 949 (1968).
[31] S. J. Luke, Ph.D. thesis, University of Washington, 1992.
[32] M. Kwato Njock, M. Maurel, H. Nifenecker, J. A. Pinston, F. Schussler, D. Barneoudand, J. Drissi, J. Kern, and J. P. Vorlet, Phys. Lett. B **207**, 289 (1988).
[33] J. Clayton *et al.*, Phys. Rev. C **45**, 1815 (1992).
[34] C. L. Tam *et al.*, Phys. Rev. C **39**, 1371 (1989).
[35] M. Kwato Njock *et al.*, Nucl. Phys. **A489**, 368 (1988).
[36] E. Migneco *et al.*, Phys. Lett. B **298**, 46 (1993).
[37] T. Reposeur *et al.*, Phys. Lett. B **276**, 418 (1992).
[38] C. A. Ogilvie *et al.*, Phys. Rev. C **40**, 654 (1989).
[39] H. Morgenstern, W. Bohne, W. Galster, K. Grabisch, and A. Kyanowski, Phys. Rev. Lett. **52**, 1104 (1984).
[40] G. S. F. Stephans *et al.*, Phys. Lett. **161B**, 60 (1985).
[41] M. Gonin, J. P. Coffin, G. Guillaume, F. Jundt, P. Wagner, P. Fintz, B. Hensch, A. Malki, A. Fahli, S. Kox, F. Merchez, and J. Mistretta, Phys. Rev. C **38**, 135 (1988).
[42] L. Pienkowski, A. Lleres, H. Nifenecker, J. Blachot, J. Crancon, A. Gizon, M. Maurel, and C. Ristori, Z. Phys. A **334**, 315 (1989).
[43] H. Morgenstern, W. Bohne, K. Grabisch, H. Zehr, and W. Stoffler, Z. Phys. A **313**, 39 (1983).
[44] S. G. Teichmann, S. B. Gazes, J. E. Mason, R. B. Roberts, and H. J. Kim, Phys. Lett. B **283**, 37 (1992).